Large molecular fluorescence enhancement by a nanoaperture with plasmonic corrugations

Heykel Aouani,[1] Oussama Mahboub,[2] Eloïse Devaux,[2] Hervé Rigneault,[1] Thomas W. Ebbesen,[2] and Jérôme Wenger[1,*]

[1]*Institut Fresnel, CNRS, Aix-Marseille University, Ecole Centrale Marseille, Campus de St Jérôme, 13397 Marseille, France*
[2]*ISIS, University of Strasbourg, CNRS, 8 allée G.Monge, 67000 Strasbourg, France*
[*]*jerome.wenger@fresnel.fr*

Abstract: We investigate the influence of circular corrugations surrounding a central nanoaperture to further enhance the fluorescence count rate per emitter and control its emission directionality. Adding a single corrugation already allows to significantly increase the fluorescence signal as compared to a bare nanoaperture. A complete fluorescence characterization quantifies the excitation and emission gains contributing to the fluorescence enhancement process as the number of corrugations is increased.

OCIS codes: (050.1220) Apertures; (240.6680) Surface plasmons; (170.6280) Spectroscopy, fluorescence and luminescence; (050.2770) Gratings; (050.6624) Subwavelength structures.

References and links

1. L. Novotny and N. H. van Hulst "Antennas for light," Nat. Photonics, **5**, 83-90 (2011).
2. Y. Fu and J. R. Lakowicz, "Modification of single molecule fluorescence near metallic nanostructures," Laser Photon. Rev. **3**, 221-232 (2009).
3. A. Kinkhabwala, Z. F. Yu, S. H. Fan, Y. Avlasevich, K. Mullen, and W. E. Moerner, "Large Single-Molecule Fluorescence Enhancements Produced by a Bowtie Nanoantenna," Nat. Photonics **3**, 654-657 (2009).
4. A. Curto, G. Volpe, T.H. Taminiau, M. Kreuzer, R. Quidant, and N. F. Van Hulst, "Unidirectional Emission of a Quantum Dot Coupled to a Nanoantenna," Science, **329**, 930-933 (2010).
5. F. J. Garcia-Vidal, L. Martin-Moreno, T. W. Ebbesen, and L. Kuipers, "Light passing through subwavelength apertures," Rev. Mod. Phys., **82**, 729-787 (2010).
6. H. J. Lezec, A. Degiron, E. Devaux, R. A. Linke, L. Martin-Moreno, F. J. Garcia-Vidal, and T. W. Ebbesen, "Beaming Light from a Subwavelength Aperture," Science, **297**, 820-822 (2002).
7. E. Laux, C. Genet, T. Skauli, and T. W. Ebbesen, "Plasmonic photon sorters for spectral and polarimetric imaging," Nat. Photonics **2**, 161-164 (2008).
8. A. Nahata, R. A. Linke, T. Ishi, and K. Ohashi, "Enhanced nonlinear optical conversion from a periodically nanostructured metal film," Opt. Lett. **28**, 423-425 (2003).
9. T. Ishi, J. Fujikata, K. Makita, T. Baba, and K. Ohashi, "Si Nano-Photodiode with a Surface Plasmon Antenna," Jap. J. Appl. Phys. **44**, L364L366 (2005).
10. O. Mahboub, S. Carretero Palacios, C. Genet, F. J. Garcia-Vidal, S. G. Rodrigo, L. Martin-Moreno, and T. W. Ebbesen, "Optimization of bulls eye structures for transmission enhancement," Opt. Express **18**, 11292-11299 (2010).
11. H. Aouani, O. Mahboub, N. Bonod, E. Devaux, E. Popov, H. Rigneault, T. W. Ebbesen, and J. Wenger, "Bright unidirectional fluorescence emission of molecules in a nanoaperture with plasmonic corrugations," Nano Lett. **11**, 637-644 (2011).
12. J. Wenger, D. Gérard, J. Dintinger, O. Mahboub, N. Bonod, E. Popov, T. W. Ebbesen, and H. Rigneault, "Emission and excitation contributions to enhanced single molecule fluorescence by gold nanometric apertures," Opt. Express **16**, 3008-3020 (2008).

#141551 - $15.00 USD Received 24 Jan 2011; revised 25 Feb 2011; accepted 27 Feb 2011; published 22 Jun 2011

13. N. Bonod, E. Popov, D. Gérard, J. Wenger, and H. Rigneault, "Field enhancement in a circular aperture surrounded by a single channel groove," Opt. Express **16**, 2276-2287 (2008).

1. Introduction

Photonic nanostructures are receiving a considerable interest to enhance and control the luminescence properties of a single quantum emitter [1–4]. In the search of deterministic and highly reproducible nanoantennas, much attention has been devoted to subwavelength apertures milled in metallic films [5]. Adding a periodic circular grating (also known as the Bull's eye structure) around the central aperture enables further control on the light-matter interaction, to improve the transmission efficiency and directionality [6, 7], enhance the non-linear conversion efficiency [8], or realize a photodiode with high-speed response [9]. An exhaustive exploration of the design parameters defining the corrugated nanoaperture is now at hand for the optical transmission process [10]. For the molecular fluorescence process, it has been demonstrated very recently that an optimized nanoaperture surrounded by 5 circular corrugations can significantly enhance the fluorescence count rates per molecule and control the emission directivity [11]. Many studies still deserve to be done to understand how the many design parameters for corrugated nanoapertures influence the fluorescence enhancement process.

In this paper, we focus on the influence of the number of circular corrugations surrounding a central nanoaperture to further enhance the fluorescence count rate per emitter. A complete fluorescence characterization combining correlation spectroscopy and lifetime measurements quantifies the excitation and emission gains contributing to the fluorescence enhancement as the number of corrugations is increased. By reciprocally coupling the far field radiation to the local energy inside the central aperture, the circular grating antenna leads to fluorescence enhancement factors significantly above those obtained with non-corrugated apertures.

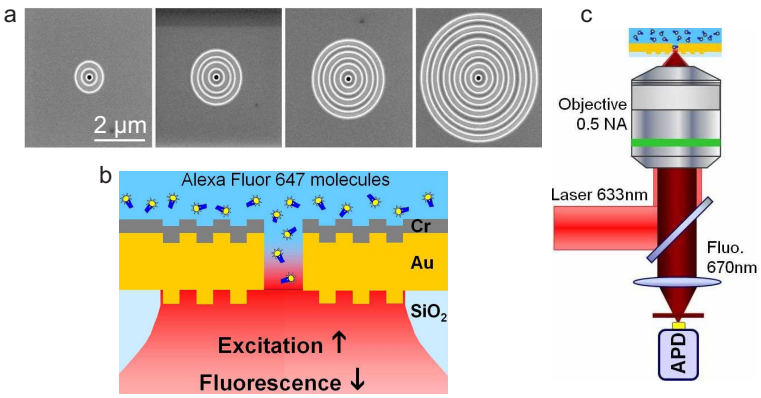

Fig. 1. (a) Scanning electron microscope image of the fabricated nanoapertures with 1, 2, 3 and 5 corrugations. (b) and (c) Experimental configuration.

2. Materials and methods

2.1. *Corrugated nanoapertures fabrication*

The preparation of the corrugated nanoapertures is based on two-step direct focused ion beam milling (FIB) [11]. First, the glass substrate is coated with a thin chromium adhesion layer and a 50 nm thick gold layer to make the substrate conductive. Periodic concentric corrugations

#141551 - $15.00 USD Received 24 Jan 2011; revised 25 Feb 2011; accepted 27 Feb 2011; published 22 Jun 2011

are milled into the glass substrate using optimized design parameters derived from reference [10]. The groove period is 440 nm, width 200 nm, depth 65 nm, and there is an increasing number of corrugations up to 5 grooves. Two layers of gold (140 nm) and chromium (60 nm) are then deposited on top of the corrugated substrate to obtain the final gold thickness with a chromium layer on top [11]. Finally, a central aperture of 140 nm diameter is opened with FIB. This diameter is chosen to provide maximum fluorescence enhancement [12]. Typical scanning electron microscopy (SEM) images of the fabricated samples are presented in Fig. 1.

2.2. *Fluorescence correlation spectroscopy to quantify the fluorescence enhancement*

Fluorescence correlation spectroscopy (FCS) is a powerful tool to count the number of emitters in a defined observation volume. FCS records the temporal fluctuations of the fluorescence signal $F(t)$, and computes its temporal correlation $G^{(2)}(\tau) = \langle F(t).F(t+\tau)\rangle / \langle F(t)\rangle^2$, where $\langle . \rangle$ stands for time-averaging. Numerical analysis of the FCS data quantifies the average number of molecule N in the observation volume (full details on the FCS analysis can be found in [12] and in the supporting information of [11], Fig. 2(a) presents a typical fluorescence correlation function and corresponding time trace). It is then straightforward to compute the fluorescence count rate per molecule *CRM* (the number of photons emitted by a molecule per second) as $CRM = \langle F(t)\rangle / N$. This enables an accurate measurement of fluorescence enhancement factors.

To distinguish the relative contributions of the excitation and emission gains in the overall fluorescence enhancement factor, we have developed a specific procedure [12]. Briefly, the fluorescence *CRM* is measured by FCS while increasing the excitation power I_e. This set of data is fitted by the standard expression of the fluorescence count rate per molecule: $CRM = AI_e/(1+I_e/I_s)$, where A is a constant proportional to the molecular absorption cross-section, emission rate and setup collection efficiency and I_s is the saturation power. In the saturation regime ($I_e \gg I_s$), $CRM = AI_s$ and the fluorescence signal does not depend anymore on the excitation. The fluorescence enhancement at saturation, which corresponds to the the ratio between the products AI_s of the fitting parameters, is equivalent to the emission gain η_{em} brought by the antenna. This emission gain η_{em} is expressed as the product of the radiative rate enhancement η_{rad} times the collection efficiency enhancement η_κ: $\eta_{em} = \eta_{rad}\eta_\kappa$. We stress that there is no need to reach practically the saturation regime, the numerical fits in Fig. 2(b) suffice to determine the saturation intensity I_s and the *CRM* asymptotic limit AI_s.

In the weak excitation regime ($I_e \ll I_s$), the fluorescence enhancement equals $\eta_F = CRM_{aperture}/CRM_{solution} = A_{aperture}/A_{solution}$. This can be specified as $\eta_F = \eta_\kappa \eta_\phi \eta_{exc}$, [1] where η_κ is the collection efficiency enhancement, η_{exc} is the excitation intensity enhancement and $\eta_\phi = \eta_{rad}/\eta_{tot}$ is the quantum efficiency enhancement (ratio of radiative rate enhancement η_{rad} to the modification of the total fluorescence decay rate η_{tot}). The alteration in the total fluorescence decay rate η_{tot} is determined separately by fluorescence lifetime measurements using the standard Time-Correlated Single Photon Counting (TCSPC) method, which is detailed in Ref. [12]. To quantify the excitation intensity gain η_{exc}, we rewrite the fluorescence enhancement as $\eta_F = \eta_{exc}\eta_{em}/\eta_{tot}$ to make apparent the emission gain η_{em}. The separate knowledge of η_F, η_{em} and η_{tot} finally quantifies the excitation intensity gain η_{exc}. This procedure separates the excitation, emission, and decay rate contributions. Please note that the emission gain η_{em} contains a term proportional to the setup collection efficiency. Therefore, the ratio $\eta_{em}/\eta_{tot} = \eta_\kappa \eta_\phi$ is greater than the quantum yield enhancement of the fluorophore [11]. More details about this procedure can be found in reference [12].

2.3. *Experimental setup*

The experimental setup (Fig, 1) uses a 0.5 NA water-immersion objective (Zeiss Neofluar). This moderate numerical aperture was chosen to realize a spot diameter in the focal plane

#141551 - $15.00 USD Received 24 Jan 2011; revised 25 Feb 2011; accepted 27 Feb 2011; published 22 Jun 2011

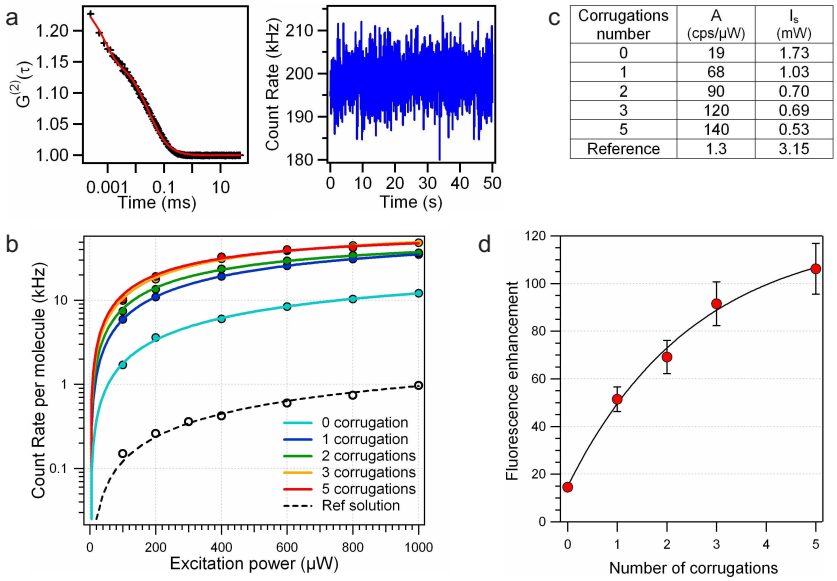

Corrugations number	A (cps/µW)	I_s (mW)
0	19	1.73
1	68	1.03
2	90	0.70
3	120	0.69
5	140	0.53
Reference	1.3	3.15

Fig. 2. (a) Typical fluorescence correlation function and fluorescence raw time trace in the case of an aperture with three corrugations and 400 μW excitation power. (b) Fluorescence count rate per molecule *CRM* versus excitation power for the different samples. (c) Parameters of the numerical fits in (b). (d) Fluorescence enhancement factors relative to the open solution, in the weak excitation regime. The line is a guide to the eyes.

of about 1.5 μm, in order to cover the circular corrugations surrounding the apertures. All experiments are performed on Alexa Fluor 647 molecules (A647, Invitrogen, Carlsbad CA, absorption / emission peaks at 650 and 672 nm) diluted in a standard water-based phosphate buffered saline (PBS) solution. For FCS, excitation is performed with a 632.8 nm CW linearly polarized laser beam, while a picosecond laser diode at 636 nm is used for fluorescence lifetime measurements. All excitation power measurements are performed at the entrance port of the confocal microscope. The backward-emitted fluorescence is detected by avalanche photodiodes with 670 ± 20 nm bandpass filters. For FCS, the fluorescence temporal fluctuations $F(t)$ are recorded by a hardware correlator (ALV6000, ALV GmbH, Langen). For fluorescence lifetime measurements, the photodiode signal is sent to a fast time-correlation counting module (PicoHarp300, Picoquant GmbH, Berlin) [12].

To analyse the angular distribution of the fluorescence radiation, we image the fluorescence intensity in the back focal plane of a 1.2 NA water immersion objective [4, 11]. By property of the back focal plane (Fourier plane), the radial coordinate in these images represents the numerical aperture $n\sin(\theta)$, where the medium refractive index is $n = 1.33$ and θ is the emission polar angle. The back focal plane images thus represent the radiation pattern for different angular directions from the antenna.

3. Experimental results and discussion

We start our investigations by determining the *CRM* while increasing the excitation power from 0.1 to 1 mW. Results as measured by FCS are presented in Fig. 2(b), together with the numerical fits according to the model $CRM = AI_e/(1+I_e/I_s)$. The fit parameters A, I_s are summarized in Fig. 2(c). Large *CRM* values are readily obtained with corrugated nanoapertures even in the case of low excitation powers below 100 μW, hereby demonstrating single molecule sensitivity

#141551 - $15.00 USD Received 24 Jan 2011; revised 25 Feb 2011; accepted 27 Feb 2011; published 22 Jun 2011

with a simple low NA lens. It is also apparent that corrugated apertures provide much higher fluorescence count rates than non-corrugated apertures, with a growing *CRM* as the number of corrugations is increased. This is a clear indication of the influence of the plasmonic corrugations surrounding the apertures. Please note that these results are highly reproducible, with a relative uncertainty of 10% on the *CRM* corresponding to the minor variations from a structure to the next and to the repeatability of measurements on our setup.

To quantify the influence of the circular corrugations, we compute the fluorescence enhancement in the low excitation limit $\eta_F = CRM_{aperture}/CRM_{solution} = A_{aperture}/A_{solution}$ (Fig. 2(d)). We observe a growing behavior of the enhancement factors as the number of corrugations is increased from 0 ($\eta_F = 14.5$) up to 5 ($\eta_F = 106$). These results deserve several comments. Firstly, the 106-fold enhancement by the aperture with 5 corrugations is remarkably the highest fluorescence enhancement reported to date for Alexa Fluor 647 molecules in solution. Secondly, we do observe a kind of saturation effect of the enhancement factor brought by adding a supplementary corrugation when the number of corrugations exceeds 3. This is a direct consequence of (i) the limited excitation spot to about 1.5 μm diameter, which brings less energy to the more distant corrugations, and (ii) increased plasmon propagation losses as the corrugation distance is increased to the central aperture. Milling 3 corrugations appears as a good compromise between fluorescence enhancement and nanofabrication complexity in the case of our setup. Thirdly, a single corrugation already provides a 3.5 times higher enhancement factor ($\eta_F = 51.5$) as compared to a bare aperture. This constitutes the first experimental observation of the effect numerically predicted in [13], and stands in good agreement with the values inferred in this reference.

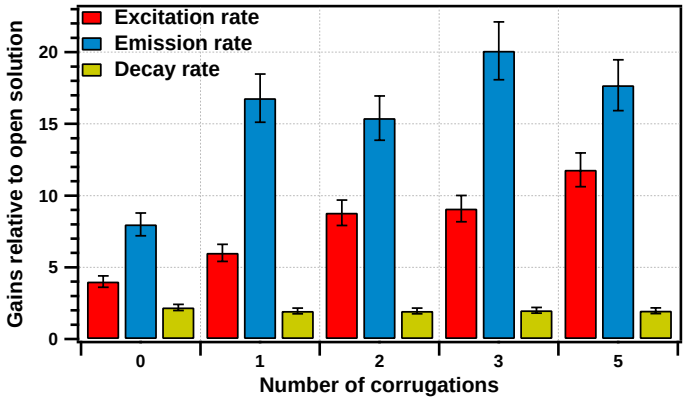

Fig. 3. Excitation η_{exc}, emission η_{em} and total decay rate η_{tot} gains contributing to the global fluorescence enhancement $\eta_F = \eta_{exc}\eta_{em}/\eta_{tot}$.

The next step determines the respective contributions of excitation and emission gains in the global fluorescence enhancement, following the procedure described in Section 2.2. Figure 3 summarizes our results for the different nanoapertures. Both excitation and emission gains are higher in the presence of corrugations than for a non-corrugated aperture. The concentric corrugations clearly improve the antenna capability of the central aperture to reversibly couple the far field radiation to near-field energy. The excitation gain gradually increases with the number of corrugations, indicating a stronger excitation energy concentration in the central aperture. The emission gain appears almost equivalent for the different numbers of corrugations. This indicates that a single corrugation already enables strong concentration of the fluorescence emission towards the detectors, as we will discuss below. This set of values forms the first com-

#141551 - $15.00 USD Received 24 Jan 2011; revised 25 Feb 2011; accepted 27 Feb 2011; published 22 Jun 2011

plete characterization quantifying the influence of the number of corrugations on the excitation and emission gains for molecular fluorescence enhancement.

To quantify the fluorescence emission angular distribution, we record the fluorescence intensity images in the back focal plane of a 1.2 NA microscope objective. Figure 4(a) presents our experimental results. For the non-corrugated aperture (N=0), the image contains a single disk representing the maximum collection angle at 64°, while for all corrugated apertures, the image contains an additional bright spot centered on the optical axis. This set of data is analyzed to display the different radiation patterns in the polar graphs in Fig. 4(b). The emission from a non-corrugated aperture is mostly limited by our collection NA, while the emission from the corrugated apertures can be tuned to high directionality in the direction normal to the sample by simply increasing the number of grooves. Starting with a single groove (N=1), the emission half width at half maximum (HWHM) is 37°, which already shows a nice control of the emission directivity. Further increasing the number of grooves narrows the angular distribution to 14° with N=2 and 10° with N=3.

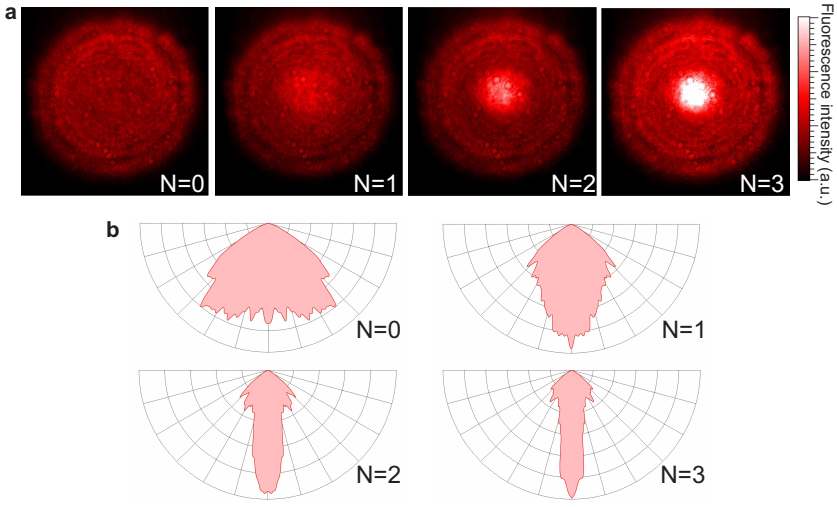

Fig. 4. (a) Fluorescence intensity distribution in the back focal plane of a 1.2 NA objective for a single nanoaperture with an increasing number N of periodic corrugations. (b) Angular radiation patterns corresponding to the images in (a).

4. Conclusion

We quantify the dependence of the fluorescence enhancement per molecule on the number of circular corrugations surrounding a nanoaperture. The circular grating antenna increases both the excitation and emission rates of single emitters diffusing inside the central aperture, leading to fluorescence enhancement factors significantly above those obtained with bare apertures. Additionally, we demonstrate efficient single molecule detection in solution with a simple low NA lens. We show that a single groove milled around a nanoaperture already provides a supplementary 3.5-fold increase in the fluorescence enhancement as compared to a bare nanoaperture, realizing the first experimental observation of the effect numerically predicted in [13]. These results and the many opportunities for further optimization [10, 13] open promising routes for ultimate control of the emission from a single quantum emitter [1].

#141551 - $15.00 USD Received 24 Jan 2011; revised 25 Feb 2011; accepted 27 Feb 2011; published 22 Jun 2011

Acknowledgments

This research is partly funded by the European Research Council under contract 227577 Plasmonics, and by the Provence-Alpes-Côte d'Azur Region.

#141551 - $15.00 USD Received 24 Jan 2011; revised 25 Feb 2011; accepted 27 Feb 2011; published 22 Jun 2011